



# Morphology of BaSO<sub>4</sub> crystals grown at the liquid–liquid interface

Debabrata R. Ray, Ashavani Kumar, Satyanarayana Reddy, S. R. Sainkar, N. R. Pavaskar and Murali Sastry\*

Materials Chemistry Division, National Chemical Laboratory, Pune – 411 08, India.  
E-mail: sastry@ems.ncl.res.in

Received 18th October 2001, Accepted 30th October 2001  
Published on the Web 7th November 2001

Paper

Barite crystals were grown at the interface between an aqueous solution of Ba<sup>2+</sup> ions and organic solutions of chloroform and hexane containing fatty acid/fatty amine molecules by reaction with sodium sulfate. The crystals grown at the interface in all cases had a nearly similar flat, plate-like morphology consistent with the barite structure. This morphology of the crystals resembles that of barite obtained during growth in solution in the presence of crystal growth inhibitors and is significantly different from that of barite crystals grown at the air–water interface. The use of interfacial effects such as dielectric discontinuity, finite solubility of the two solvents, *etc.*, opens up exciting possibilities for tailoring the morphology of crystals at the liquid–liquid interface.

## Introduction

Development of protocols to grow crystals of controllable structure, size, morphology and superstructures of pre-defined organizational order is an important goal in crystal engineering with tremendous implications in the ceramics industry.<sup>1,2</sup> Lured by the exquisite control that biological organisms exert over mineral nucleation and growth (both amorphous and crystalline) by a process known as biomineralization,<sup>3,4</sup> materials scientists are trying to understand biomineralization and, thereby, develop biomimetic approaches for the synthesis of advanced ceramic materials. It is now established that an important requirement for biomineralization is epitaxy between the crystal nucleating face and underlying bio-organic surface and, consequently, biomimetic surfaces such as those presented by Langmuir monolayers,<sup>5,6</sup> self-assembled monolayers (SAMs) on planar<sup>7</sup> and nanoscale curved surfaces<sup>8</sup> as well as functionalized polymer surfaces<sup>9</sup> have been studied in great detail. Attempts have also been made to control the morphology of crystals *via* addition of suitable crystallization inhibitors<sup>10</sup> and carrying out crystal growth in constrained environments such as those afforded by microemulsions.<sup>11</sup> Very recently, some of us have shown that the growth of SrCO<sub>3</sub> in thermally evaporated fatty acid bilayer stacks resulted in an unusual flower-like assembly of strontianite needles.<sup>12</sup>

The liquid–liquid interface is an important area of research in chemistry that impacts understanding of the stability of emulsions, chemical separation processes, interfacial catalysis as well as many processes in biological systems.<sup>13</sup> Only recently has the liquid–liquid interface been viewed seriously as a medium for the organization of micron sized objects<sup>14</sup> and growth of nanoparticles of CdS.<sup>15</sup> To the best of our knowledge, there are no reports in the literature on the use of the liquid–liquid interface in the biomimetic growth of minerals. In this communication, we address this lacuna and investigate the growth of BaSO<sub>4</sub> (barite) crystals at the interface between an aqueous solution of Ba<sup>2+</sup> ions and organic solutions of chloroform and hexane containing fatty acid/fatty amine molecules by reaction with sodium sulfate. The process is seemingly similar to the growth of BaSO<sub>4</sub> crystals at the air–water interface with anionic Langmuir monolayers as the template<sup>6</sup> with the following important differences. The magnitude of the dielectric discontinuity

between water–organic solution and water–air would be different and could lead to important differences in the electrostatics of complexation of the Ba<sup>2+</sup> ions with the anionic surfactant molecules at the interface. Furthermore, the finite solubility of the two solutions would lead to a region of the interface with a much broader gradation in the dielectric function which would in turn influence the electrostatics of the metal ion complexation with the lipid molecules as well as the organization of the templating lipid molecules in the interfacial region. The solvation of the hydrocarbon chains in the organic phase would also contribute to disruption in the ordering of the surfactant molecules at the water–organic solution interface with important consequences in the epitaxy associated with crystal nucleation processes.

## Experimental details

Stearic acid, octadecylamine, hexane, chloroform, barium chloride and sodium sulfate were obtained from Aldrich Chemicals and used without further purification.

A 50 mL solution of 10<sup>−2</sup> M stearic acid in chloroform was taken in a separating funnel and 50 mL of 10<sup>−2</sup> M aqueous solution of BaCl<sub>2</sub> (pH = 6.2) was added. The biphasic mixture was allowed to rest for 30 minutes following which 15 mL of a 10<sup>−2</sup> M aqueous solution of Na<sub>2</sub>SO<sub>4</sub> was injected slowly into the aqueous side of the chloroform–water interface (solubility of CHCl<sub>3</sub> in water is 0.08% w/w; dielectric constant = 4.8; density = 1.47 g mL<sup>−1</sup>). This leads to a supersaturation ratio of *ca.* 400 in the salt solution. As the injection of Na<sub>2</sub>SO<sub>4</sub> progressed, the interface turned turbid and after some time it was noticed that crystals of BaSO<sub>4</sub> were formed at the liquid–liquid interface. Apart from the interface, the organic and aqueous phases were clear. The organic solution was carefully removed from the separating funnel and the crystals separated by filtration, washed with copious amounts of double distilled water and placed on Si(111) substrates for scanning electron microscopy (SEM) and X-ray diffraction (XRD) measurements. In a similar manner, the crystallization of BaSO<sub>4</sub> was also carried out using octadecylamine in chloroform as well as stearic acid in hexane (solubility of hexane in water is 0.001% w/w; dielectric constant = 1.9; density = 0.66 g mL<sup>−1</sup>).

In control experiments, the crystallization of BaSO<sub>4</sub> was

accomplished in a 50 mL chloroform/hexane (without stearic acid)–50 mL BaCl<sub>2</sub> biphasic mixture by injection of 15 mL of 10<sup>−2</sup> M aqueous solution of Na<sub>2</sub>SO<sub>4</sub>. The crystals were formed predominantly in the bulk of the aqueous solution and slowly settled down at the interface in the case of chloroform (please note: since the density of chloroform is greater than that of water, the aqueous component rests on top of the organic solution and the crystals formed in the aqueous phase settle under the influence of gravity at the interface) and at the bottom of the reaction vessel in the case of hexane. The crystals formed at the water–organic solvent interface in the control experiments were also examined by SEM. In order to facilitate comparison of the morphology of BaSO<sub>4</sub> crystals formed at the liquid interface with the morphology reported in the literature for crystals grown at the air–water interface at considerably lower supersaturation ratios,<sup>6b</sup> the crystallization experiments with stearic acid in hexane were performed at a supersaturation ratio of *ca.* 50 by adjusting the amount of Na<sub>2</sub>SO<sub>4</sub> solution (concentration = 1.41 × 10<sup>−4</sup> M) injected into the BaCl<sub>2</sub> aqueous solution. In this experiment, crystal growth at the interface was extremely slow and the crystals were harvested for analysis after 12 h of reaction. In all the crystallization experiments, the temperature of the biphasic solutions was held at 25 °C.

XRD analysis of all the BaSO<sub>4</sub> samples was carried out on a Philips PW 1830 instrument operating in the transmission mode at 40 kV voltage and a current of 30 mA with CuK<sub>α</sub> radiation. SEM measurements were carried out on a Leica Stereoscan-440 scanning electron microscope (SEM) equipped with a Phoenix EDAX attachment.

## Results and discussion

The amphiphilic nature of the stearic acid molecules would lead to their adsorption at the liquid–liquid interface and enable electrostatic complexation of Ba<sup>2+</sup> ions with the carboxylate groups of the fatty acid in a manner akin to that observed in Langmuir monolayers at the air–water interface.<sup>6</sup> The concentration of divalent metal ions near Langmuir monolayers of fatty acids is known to be 4–5 orders of magnitude larger than the concentration in the bulk of the aqueous solution leading to a high supersaturation ratio at the interface<sup>16</sup> and it is expected that a similar metal ion concentration enhancement would occur at the hexane–water interface (and the chloroform–water interface) as well. Thereafter, reaction of the Ba<sup>2+</sup> ions with sulfate anions leads to the formation of BaSO<sub>4</sub> at the liquid–liquid interface. Fig. 1 shows the SEM micrographs at different magnifications obtained from the BaSO<sub>4</sub> crystals grown at the interface between hexane and water with stearic acid in the hexane phase. At lower magnification (Fig. 1A), a number of BaSO<sub>4</sub> crystals of uniform size are observed. Spot profile EDAX measurements taken from within one of the crystals yielded a Ba : S : O ratio in excellent agreement with that expected for barite. Some crystals fortuitously oriented perpendicular to the Si(111) substrate can also be seen in the figure. It is clear from this image that the

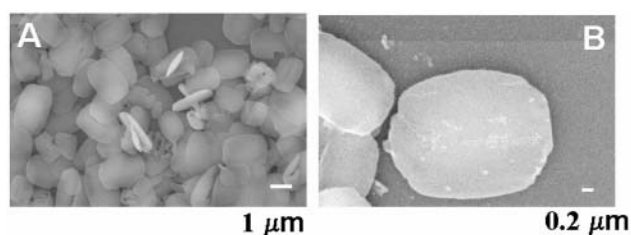


**Fig. 1** A and B – SEM micrographs at different magnifications recorded from BaSO<sub>4</sub> crystals grown at the water–hexane interface with stearic acid molecules in the organic phase.

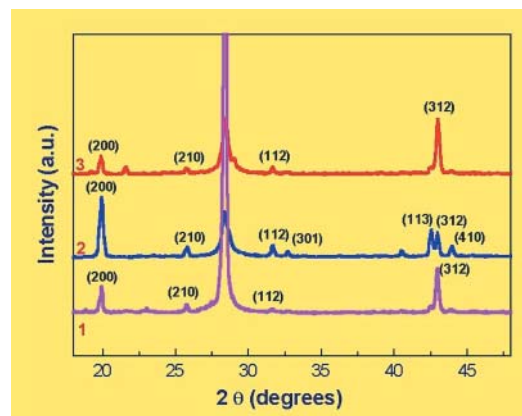
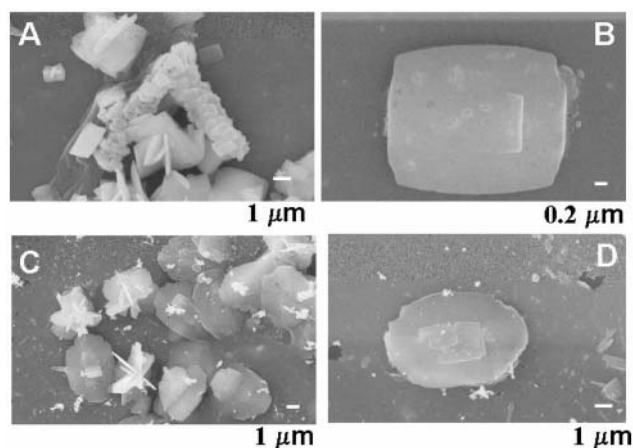


**Fig. 2** XRD patterns recorded from BaSO<sub>4</sub> crystals grown at the water–hexane interface with stearic acid in the organic phase (curve 1); at the water–chloroform interface with octadecylamine in the organic phase (curve 2) and at the water–chloroform interface with stearic acid in the organic phase (curve 3).

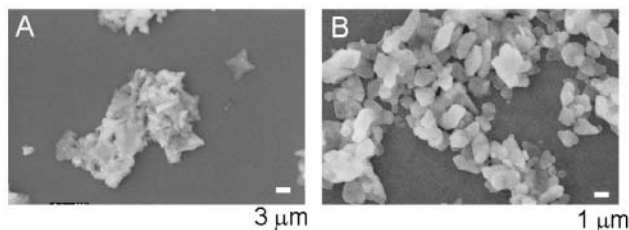
particles are quite flat and plate-like in overall morphology. The higher magnification SEM picture shown in Fig. 1B clearly reveals the well-rounded and nearly circular shape of an individual crystal. The XRD pattern recorded for this film is shown as curve 1 in Fig. 2. The XRD pattern was indexed with reference to the unit cell of the barite structure ( $a = 8.87$  Å,  $b = 5.45$  Å,  $c = 7.15$  Å; space group *Pnma*).<sup>17</sup>

Fig. 3 shows SEM images of BaSO<sub>4</sub> crystals grown at the water–chloroform interface with stearic acid (images A and B) and octadecylamine (images C and D) as the templating molecules in the organic phase. In the case of octadecylamine, the molecules at the interface would be positively charged at pH = 6.2 and therefore, the sulfate ions would be bound at the interface rather than Ba<sup>2+</sup> ions as was the case with stearic acid molecules. We were interested in seeing whether the order of complexation of the ionic species prior to crystallization affected the morphology of the barite crystals grown at the liquid–liquid interface. As mentioned earlier, chloroform is denser than water and therefore the orientation of both the stearic acid and octadecylamine molecules at the liquid–liquid interface would be opposite to that in the case of water–hexane.

As in the case of barite crystals grown at the water–hexane interface (Fig. 1), the BaSO<sub>4</sub> crystals grown at the chloroform–water interface with both stearic acid and octadecylamine are flat and plate-like (Fig. 3). In the case of stearic acid in chloroform, unusual aggregation of the plate-like crystals had occurred to yield a cylindrical superstructure as shown in the



**Fig. 3** A and B – SEM images of BaSO<sub>4</sub> crystals grown at the interface between water and chloroform, the organic phase containing stearic acid. C and D – SEM images of BaSO<sub>4</sub> crystals grown at the water–chloroform interface, the organic phase containing octadecylamine.



**Fig. 4** A and B – SEM images recorded from  $\text{BaSO}_4$  crystals grown at the interface between water and chloroform, the organic phase containing stearic acid. The aggregated, supercrystal structure can be seen in both images at different magnifications.

centre of Fig. 3A. Such a structure was not observed in any of the other samples and was seen repeatedly, albeit sporadically, in the case of barite crystals grown using stearic acid in chloroform. Some additional aggregated  $\text{BaSO}_4$  structures imaged from such samples are shown in Fig. 4. The XRD patterns recorded from the crystals grown at the water–chloroform interface with octadecylamine and stearic acid are shown as curves 2 and 3 respectively in Fig. 2. It is clear that crystallization of barite has occurred in both cases.

The observation that flat, nearly circular barite crystals are formed at the water–organic solution interface irrespective of whether cationic or anionic lipid molecules are used is surprising and indicates a possibly minor role for the additive in determining the morphology of the crystals formed. In order to clarify this issue, SEM images at different magnifications of barite crystals grown in the control experiments with chloroform (without stearic acid in the organic solvent) were recorded and are shown in Fig. 5. The morphology of the crystals was identical in the case of the hexane experiment and for brevity these images are not shown. In the control experiment, the crystal morphology is very different from that observed when stearic acid is present in the organic phase (Figs. 1 and 3), the crystals exhibiting a star-like structure (Figs. 5A and B). Clearly, the presence of both stearic acid and octadecylamine monolayers at the water–organic solvent interface plays an important role in determining the morphology of the barite crystals formed.

While it may initially appear that the organization of stearic acid (and indeed octadecylamine) at the water–hexane/chloroform interface is similar to that of the fatty lipids at the air–water interface, there are important differences as briefly pointed out in the introduction. We would like to point out that the morphology of the barite crystals of this study is markedly different from those observed by others at the air–water interface.<sup>6</sup> Taking the specific example of barite crystals grown at the air–water interface with Langmuir monolayers of n-eicosyl sulfate and eicosanoic acid,<sup>6b</sup> this difference in morphology of the crystals could be due to the large difference in supersaturation ratios in the two studies (400 in this study *versus* 30 in ref. 6b). We therefore repeated the  $\text{BaSO}_4$  crystallization experiments with stearic acid in hexane at a supersaturation ratio of 40 as described in the experimental section. Fig. 6 shows the SEM images obtained from barite

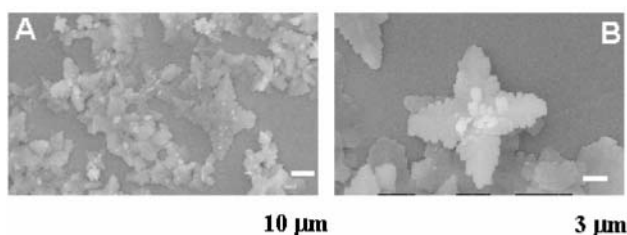


**Fig. 5** A and B – SEM images of  $\text{BaSO}_4$  crystals grown in a biphasic mixture of chloroform (without ionizable surfactant) and water in the control experiment.

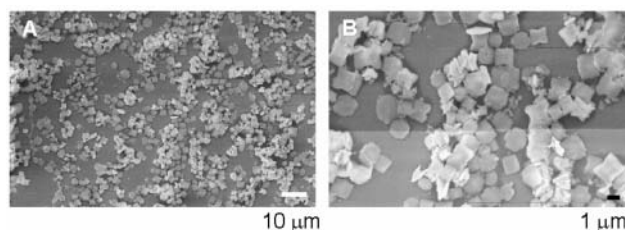


**Fig. 6** A and B – SEM images recorded from barite crystals grown at the interface between water and hexane with stearic acid in the organic phase at a supersaturation ratio of *ca.* 50.

crystals harvested from the liquid–liquid interface of this experiment. It is observed from these SEM images that the  $\text{BaSO}_4$  crystals still possess a plate-like and very flat, circular morphology even at such relatively lower supersaturation ratios. The insensitivity of the barite crystal morphology to the nature of the surfactant (cationic or anionic) as well as the supersaturation ratio is a salient feature of this study.

The morphology of the barite crystals of this study grown in the presence of cationic or anionic surfactants more closely resembles barite crystals grown in solution in the presence of crystallization inhibitors possessing (iminodimethylene)phosphonate motifs<sup>10a</sup> and inhibitors such as aminocarboxylate chelating precursors (nitrilotriacetic acid, to be more specific).<sup>10c</sup> It appears that the fatty lipid molecules at the liquid–liquid interface behave similarly to such crystal growth inhibitors. This may be a consequence of the finite solubility of the two solutions leading to a fairly broad interfacial region where the fatty lipid molecules are relatively evenly distributed. This would enable the lipid molecules to bind to nascent crystals growing at the interface and thereby control the growth of specific crystallographic faces and the crystal morphology. The electrostatic interaction between the  $\text{Ba}^{2+}$  ions and the fatty acid molecules would also be modulated by the lower dielectric constant of the organic component within the interfacial region. While the exact details of the mechanism for morphology variation of barite crystals at the liquid–liquid interface need to be worked out, it is clear that the use of such interfaces provides exciting possibilities for tailoring the growth mode of crystals.

A comparison of the higher magnification SEM images of the barite crystals grown at the water–chloroform interface with stearic acid (Figs. 3A and B) and octadecylamine (Figs. 3C and D) shows that the crystal morphology is more rounded in the case of fatty amine molecules at the interface (morphology similar to barite crystals grown at the hexane–water interface with stearic acid, Fig. 1B). Secondary nucleation can clearly be observed on the surface of the crystals in both cases. This behaviour is analogous to that observed by Bromley *et al.*<sup>10a</sup> who reported that the [100] direction curvature became more pronounced with increasing concentration of specific (iminodimethylene)phosphonates in solution thus leading to a more spherical crystal morphology.

In conclusion, it has been shown that barite crystals may be grown at the liquid–liquid interface with suitable surfactants adsorbed at the interface. The crystals exhibit a morphology not normally observed in the analogous air–water interface growth experiments. The use of the liquid–liquid interface throws open the exciting possibility of tailoring the physical and chemical properties of the interface and thereby modifying the morphology of the crystals nucleating and growing at the interface.

## References

- 1 A. H. Heuer, D. J. Fink, V. J. Laraia, J. L. Arias, P. D. Calvert, K. Kendall, G. L. Messing, J. Blackwell, P. C. Rieke,



- D. H. Thomason, A. P. Wheeler, A. Veis and A. I. Caplan, *Science*, 1992, **255**, 1098.
- 2 B. C. Bunker, P. C. Rieke, B. J. Tarasevich, A. A. Campbell, G. E. Fryxell, G. L. Graff, L. Song, J. Liu, J. W. Wirdem and G. L. McVay, *Science*, 1994, **264**, 48.
  - 3 (a) *Biomineralization, Chemical and Biochemical Perspectives*, eds. S. Mann, J. Webb and R. J. P. Williams, VCH Weinheim, 1989; (b) S. Mann, *Inorganic Materials*, eds. D. W. Bruce and D. O'Hare, John Wiley & Sons, 1996, p. 255; (c) S. Mann, *J. Chem. Soc., Dalton Trans.*, 1993, 1; (d) S. Mann, *J. Chem. Soc., Dalton Trans.*, 1997, 3953.
  - 4 (a) L. Addadi and S. Weiner, *Angew. Chem., Int. Ed. Engl.*, 1992, **31**, 153; (b) S. Weiner and L. Addadi, *J. Mater. Chem.*, 1997, **7**, 689; (c) K. M. McGrath, *Adv. Mater.*, 2001, **13**, 989.
  - 5 B. R. Heywood and S. Mann, *Adv. Mater.*, 1994, **6**, 9 and references therein.
  - 6 BaSO<sub>4</sub>: (a) B. R. Heywood and S. Mann, *Langmuir*, 1992, **8**, 1492; (b) B. R. Heywood and S. Mann, *J. Am. Chem. Soc.*, 1992, **114**, 4681; CaCO<sub>3</sub>: (c) A. L. Litvin, S. Valiyaveetil, D. L. Kaplan and S. Mann, *Adv. Mater.*, 1997, **9**, 124; (d) P. J. J. A. Buijnsters, J. J. J. M. Donners, S. J. Hill, B. R. Heywood, R. J. M. Nolte, B. Zwanenburg and N. A. J. M. Sommerdijk, *Langmuir*, 2001, **17**, 3623.
  - 7 CaCO<sub>3</sub>/SrCO<sub>3</sub>: (a) J. Kuther, G. Nelles, R. Seshadri, M. Schaub, H.-J. Butt and W. Tremel, *Chem. Eur. J.*, 1998, **4**, 1834; CaCO<sub>3</sub>: (b) J. Aizenberg, A. J. Black and G. M. Whitesides, *J. Am. Chem. Soc.*, 1999, **121**, 4500.
  - 8 (a) M. Nagtegaal, R. Seshadri and W. Tremel, *Chem. Commun.*, 1998, 2139; (b) J. Kuther, R. Seshadri, G. Nelles, H.-J. Butt, W. Knoll and W. Tremel, *Adv. Mater.*, 1998, **10**, 401; (c) J. Kuther, R. Seshadri, G. Nelles, W. Assenmacher, H.-J. Butt, W. Mader and W. Tremel, *Chem. Mater.*, 1999, **11**, 1317.
  - 9 (a) S. Feng and T. Bein, *Science*, 1994, **265**, 1839; (b) G. Falini, M. Gazzano and A. Ripamonti, *Adv. Mater.*, 1994, **6**, 46.
  - 10 BaSO<sub>4</sub>: (a) L. A. Bromley, D. Cottier, R. J. Davey, B. Dobbs, S. Smith and B. R. Heywood, *Langmuir*, 1993, **9**, 3594; (b) L. Qi, H. Coffen and M. Antonietti, *Angew. Chem., Int. Ed.*, 2000, **39**, 604; (c) M. Uchida, A. Sue, T. Yoshioka and A. Okuwaki, *CrystEngComm*, 2001, **5**.
  - 11 BaSO<sub>4</sub>: (a) J. D. Hopwood and S. Mann, *Chem. Mater.*, 1997, **9**, 950; (b) M. Li and S. Mann, *Langmuir*, 2000, **16**, 7088.
  - 12 M. Sastry, A. Kumar, C. Damle, S. R. Sainkar, M. Bhagwat and V. Ramaswamy, *CrystEngComm*, 2001, **21**.
  - 13 J. Bowers, A. Aarbakhsh, J. R. P. Webster, L. R. Hutchings and R. W. Randall, *Langmuir*, 2001, **17**, 140.
  - 14 N. Bowen, F. Arias, T. Deng and G. M. Whitesides, *Langmuir*, 2001, **17**, 1757.
  - 15 S. D. Sathaye, K. R. Patil, D. V. Paranjape, A. Mitra, S. V. Awate and A. B. Mandale, *Langmuir*, 2000, **16**, 3487.
  - 16 J. N. Israelachvili, *Intermolecular and Surface Forces*, Academic Press, New York, 1997, ch. 12, p. 237.
  - 17 S. E. Redfern and S. C. Parker, *J. Chem. Soc., Faraday Trans.*, 1998, **94**, 1947.